Synthetic hydrogels as scaffolds to manipulate endothelium cell behaviors

Yong Mei Chen[ab]*, Jing Jing Yang[b], Yoshihito Osada[c], Jian Ping Gong[b]*

[a]MOE Key Laboratory for Non-equilibrium Condensed Matter and Quantum Engineering, Biomedical Engineering and Biomechanics Center, Department of Chemistry, School of Science, Xi'an Jiaotong University, Xi'an 710049, P. R. China.

[b]Faculty of Advanced Life Science, Hokkaido University, Sapporo 060-0810, Japan

[c]RIKEN 2-1, Hirosawa, Wako, Saitama 351-0198, Japan

*Corresponding authors: Y. M. Chen, chenym@mail.xjtu.edu.cn , Tel: 86-29-8266-5488，Fax: 86-29-8266-3914, J. P. Gong, gong@sci.hokudai.ac.jp, Tel & Fax: 81-11-706-2774.

Abstract

Synthetic hydrogels can be used as scaffolds that not only favor endothelial cells (ECs) proliferation but also manipulate the behaviors and functions of the ECs. In this review paper, the effect of chemical structure, Young's modulus (*E*) and zeta potential (ζ) of synthetic hydrogel scaffolds on static cell behaviors, including cell morphology, proliferation, cytoskeleton structure and focal adhesion, and on dynamic cell behaviors, including migration velocity and morphology oscillation, as well as on EC function such as anti-platelet adhesion, are reported. It was found that negatively charged hydrogels, poly(2-acrylamido-2-methylpropanesulfonic sodium) (PNaAMPS) and poly(sodium *p*-styrene sulphonate) (PNaSS), can directly promote cell proliferation, with no need of surface modification by any cell-adhesive proteins or peptides at the environment of serum-containing medium. In addition, the Young's modulus (*E*) and Zeta potential (ζ) of hydrogel scaffolds are quantitatively tuned by copolymer hydrogels, poly(NaAMPS-*co*- DMAAm) and poly(NaSS-*co*-DMAAm), in which the two kinds of negatively charged monomers NaAMPS and NaSS are copolymerized with neutral monomer, N, N-dimethylacrylamide (DMAAm). It was found that the critical Zeta potential of hydrogels manipulating EC morphology, proliferation, and motility is $\zeta_{critical}$ = — 20.83 mV and $\zeta_{critical}$ = — 14.0 mV for poly(NaAMPS-*co*-DMAAm) and poly(NaSS-*co*-DMAAm), respectively. The above mentioned

EC behaviors well correlate with the adsorption of fibronectin, a kind of cell-adhesive protein, on the hydrogel surfaces. Furthermore, adhered platelets on the EC monolayers cultured on the hydrogel scaffolds obviously decreases with an increase of the Young's modulus (E) of the hydrogels, especially when E > 60 kPa. Glycocalyx assay and gene expression of ECs demonstrate that the anti-platelet adhesion well correlates with the EC-specific glycocalyx. The above investigation suggests that understanding the relationship between physic-chemical properties of synthetic hydrogels and cell responses is essential to design optimal soft & wet scaffolds for tissue engineering.

Keywords: Synthetic hydrogel, scaffold, endothelial cell, cell behavior

1. Introduction

In order to survive and proliferation, anchorage dependent cells must adhere to and spread on a scaffold. *In vivo*, multicellular organisms composed of many kinds of anchorage dependent cells, and the scaffolds supporting the cells are either other co-surviving cells or extracellular matrix (ECM) [1,2] with an elastic modulus of *ca.* 10 kPa [3]. For example, endothelial cell (EC) monolayers are supported by the ECM secreted by vascular smooth muscle cells (VSMCs), while the VSMCs are supported by type I collagen [4]. A hydrogel, comprising of a three-dimensional (3D) network and containing more than 90% water, is the most appealing material for tissue engineering, due to its soft & wet nature that is similar to the macromolecular-based ECM in living tissue. It is naturally considered that if cells are cultivated on the hydrogel scaffolds that have viscoelastic 3D structure similar to ECM, the cells will live in the environment that is more similar to living body than on other hard and dry scaffolds, such as glass and tissue culture polystyrene (TCPS).

Over the past 10 years, there is a dramatic increase in the studies of cell behaviors on the synthetic hydrogels. This is because: (i) their structural and physic-chemical properties, such as Young′s modulus and charge density can be easily adjusted and controlled, (ii) they have a superb optical quality that is suitable for microscopic observation, and (iii) free of infection, withstand high-temperature sterilization, and relatively low cost. Furthermore, the simple and

well-defined chemical structure and high purity of synthetic hydrogels make it relatively easier for explaining the mechanism of interaction between cultured cell and scaffolds [5,6].

Even though the amazing physical-chemical properties of synthetic hydrogels that attract scientists to design hydrogels suitable for cell culture scaffolds, comparing with the commercially available naturally derived collagen gel and Matrigel^{TM} (a mixture of murine sarcoma-derived ECM) [7], cell proliferation does not occur spontaneously on many neutral synthetic hydrogels, which is one of the significant disadvantages as cell cultivation scaffold. For example, polyacrylamide (PAAm), poly(ethylene oxide) (PEO) and polyacrylamide (PVA) show a poor cellular viability without modification with cell-adhesive proteins or peptides (collagen, laminin, fibronectin, RGD sequence) [8-16].

Recently, we have reported that ECs from human, i.e., human umbilical vein endothelial cells (HUVECs) and human coronary artery endothelial cell (HCAECs), as well as from bovine, i.e., bovine fetal aorta endothelial cells (BFAECs), could spread, proliferate, and reach confluent on the negatively charged hydrogels that are not modified by any cell adhesive proteins or peptides, such as poly(2-acrylamido-2-methylpropanesulfonic sodium) (PNaAMPS), poly(sodium p-styrene sulphonate) (PNaSS), and poly(acrylic acid) (PAA)[17]. EC is a kind of special cell covered on the inner wall of blood vessel as a monolayer, the cells play a wide variety of critical roles in the control of vascular function, such as blood vessel formation and inhibition of platelet adhesion [18-22]. Therefore, the relationship between the physic-chemical properties of the synthetic hydrogels and the behaviors of EC has been further investigated.

In this review, our recent progresses on manipulate EC behaviors and functions by the physic-chemical properties of the synthetic hydrogels, including the effect of chemical structure of the hydrogels on cell proliferation behavior and platelet adhesion on the cultured EC monolayer, effect of Zeta potential of hydrogels on static cell behaviors, including cell morphology, proliferation, cytoskeletal structure and focal adhesion, and on dynamic cell behaviors, including migration velocity and morphology oscillation, as well as on EC function, anti-platelet adhesion, will be introduced.

2. Manipulation EC behaviors

According to our originally established method, the ECs are directly cultured on the surface of hydrogels that are not modified by any cell-adhesive proteins or peptides before cell cultivation.

Thus, it is easy to discuss the correlation between the properties of the synthetic hydrogels, including the chemical structure, Young's modulus and Zeta potential (ζ), and the cell properties and behaviors.

2.1 Effect of chemical structure of hydrogels on cell proliferation

The synthetic hydrogels used for the scaffolds of ECs are classified into 3 categories, that is, neutral, negatively charged weak polyelectrolyte, and strongly charged negative polyelectrolyte hydrogels [17]. The neutral hydrogels have no ionized group, including PVA, PDMAAm, and PAAm; the weakly charged hydrogels have carboxylic acid groups on the side chains of the polymers and they are pH-dependent, including PAA and PMAA; the strongly charged hydrogels have sulfonate groups on the side chains of the polymers, and they are fully dissociated, including PNaAMPS and PNaSS. The molecular structures of these hydrogels and the typical phase-contrast micrographs of BFAECs cultured for 120 h on these hydrogels with various cross-linker concentrations M (mol% in relative to the monomer concentration) , i.e., PAAm (2 mol%), PDMAAm (4 mol%), PVA (6 mol%), PAA (2 mol%), PMAA (1 mol%), PNaAMPS (6 mol%), and PNaSS (10 mol%), are shown in Figure 1.

After a prolonged culture time, the cell morphology and proliferation strongly depend on the chemical structure of the hydrogels (Figure 1 column V). Figure 2 shows the proliferation kinetics of BFAECs cultured on the various kinds of synthetic hydrogels, as well as on a control, type I collagen hyderogel. In the case of neutral hydrogels, all adhered ECs exhibit a round morphology on PAAm and PDMAAm hydrogels, indicating the ECs could not spread and proliferate on the neutral PAAm-based hydrogels. However, *c.a.* 50% of adhered ECs spread with a few irregular protrusions on the PVA hydrogel after 6 h of cultivation, and the spread ECs proliferate to a cell density of 3.5×10^4 after 144 h. It demonstrates that the cell compatibility of the PVA gel is better than that of PAAm and PDMAAm hydrogels. In addition, the cell adhesion and proliferation behavior are not obviously dependent on the cross-linker concentration, M , of the above neutral hydrogels.

In the case of the weakly charged hydrogels, *c.a.* 40% adhered ECs spread with a few irregular protrusions on the PMAA hydrogel (M = 1) after 6 h, and the spread cells proliferate to a cell density of 3.5×10^4 after 144 h. On the other hand, *c.a.* 60% adhered ECs spread with a fusiform or polygonal shape on the PAA hydrogel (M = 2), and the spread ECs proliferate to a cell

density of 3.7×10^4 after 144 h [24]. The above results demonstrate that the ECs only reach sub-confluent on the weakly negatively charged hydrogels. However, it should be mentioned that the ECs could not proliferate when the *M* of PMAA and PAA increases to more than 4 mol% (data not shown).

On the strongly charged hydrgels, more than 90% adhered ECs spread with a fusiform or polygonal shape, and the ECs proliferate to confluent with a cell density of 1.32×10^5 and 1.12×10^5 on PNaAMPS (*M* = 2) and PNaSS (*M* = 4) hydrogels, respectively, after 144 h. Although the proliferation rate of the PNaAMPS and PNaSS hydrogels are lower than that of type I collagen gel (Figure 2), the densities of the proliferated cells at confluent cultured on the two kinds of strongly charged hydrogels are comparable to those on collagen gel. The above results demonstrate that the synthetic hydrogels facilitate EC proliferation in the following order: strongly charged gels (PNaAMPS, PNaSS) > weakly charged gels (PAA, PMAA) > neutral gels (PVA, PAAm, PDMAAm).

2.2 Effect of Zeta potential on cell behaviors

The effect of chemical structure on EC proliferation indicates that the strongly charged hydrogels facilitate cell proliferation, and the charge density of hydrogel is an important parameter for controlling EC fate. Based on the above result, the effect of charge density of hydrogel on cell behaviors was systematically investigated by synthesizing copolymer hydrogels with different charge density. The copolymer hydrogels, poly(NaAMPS-*co*- DMAAm) and poly(NaSS-*co*-DMAAm), could be synthesized by combination of strongly charged moiety, PNaAMPS or PNaSS, on which ECs can proliferate very well, with a neutral moiety, PDMAAm, on which ECs cannot proliferate. The Zeta potential, ζ, of the poly(NaAMPS-*co*-DMAAm) and poly(NaSS-*co*-DMAAm) hydrogels was quantitatively tuned by adjusting the molar fraction (F) of the negatively charged NaAMPS and NaSS in the copolymer hydrogels. Because NaAMPS and NaSS are monomers with negative charge, the ζ of poly(NaAMPS-*co*-DMAAm) and poly(NaSS-*co*-DMAAm) copolymer hydrogels should be negative except F=0. Thus, a large absolute value of Zeta potential, $|\zeta|$, denotes high charge density of the copolymer hydrogels. The static cell behaviors, including cell morphology, proliferation, cytoskeleton structure, focal adhesion, as well as dynamic cell behaviors,

including migration velocity, migration distance and morphology oscillation, have been investigated on the poly(NaAMPS-*co*-DMAAm) and poly(NaSS-*co*-DMAAm) copolymer hydrogels. Furthermore, the correlation between the adsorption of fibronectin, a kind of typical cell-adhesive protein, on hydrogel surface and cell behavior was furthermore analyzed.

2.2.1 Effect of Zeta potential on static cell behaviors

Table 1 shows the degree of swelling (*q*) of HEPES buffer-equilibrated poly(NaAMPS-*co*-DMAAm) hydrogels as a function of F. It shows that *q* increases with an increase of F, due to the introduction of more sulfonate group of PNaAMPS in the copolymer hydrogels. Figure 3 shows the F as a function of $|\zeta|$ of HEPES buffer-equilibrated poly(NaAMPS-*co*-DMAAm) hydrogels. It shows that with the increase of F, the $|\zeta|$ of poly (NaAMPS-*co*-DMAAm) hydrogels increases and saturates to 30.0 mV at F = 1, confirming that the charge density of poly(NaAMPS-*co*-DMAAm) hydrogels increases with an increase of the amount of NaAMPS. It should be note that although PDMAAm is neutral, it shows a small negative ζ in HEPES buffer solution, perhaps due to its ionic adsorption in the buffer solution [25].

Typical phase-contrast micrographs of BFAECs and HUVECs cultured for 120 h on the poly (NaAMPS-*co*-DMAAm) hydrogels with various $|\zeta|$ are shown in Figure 4. To reveal the correlation between $|\zeta|$ and cell proliferation behavior, the cell density cultured for 120 h of two kinds of ECs, BFAEC and HUVEC, as a function of the $|\zeta|$ of the poly (NaAMPS-*co*-DMAAm) hydrogels, is plotted (Figure 5).

In the case of BFAECs, it shows that there are three stages of cell density change with an increase of the $|\zeta|$. When $|\zeta| \leq 16.26$ mV (F ≤ 0.3), the cell density slowly increases with an increase of the $|\zeta|$. This stage is denoted as slowly increase stage. At this stage, the cells exhibit a round morphology or slight spreading with a few irregular protrusions at 120 h, and the cell density is lower than 2.0×10^4 cell/cm^2. When $|\zeta| = 20.83$ mV (F = 0.4), the cell density obviously increases with an increase of the $|\zeta|$. This stage is denoted dramatically increase stage. In this stage, all of the cells spread extensively on the hydrogel, and the cells proliferate to form a confluent monolayer with a cell density of 1.4×10^5 cell/cm^2 at 120 h. Furthermore, when

$|\zeta|$ > 20.83 mV (F > 0.4), the cell density does not obviously dependent on the $|\zeta|$, and saturates to a stable value. This stage is denoted as stable stage. At this stage, the cells proliferate to form a confluent monolayer with a cell density of *c.a.*1.4×10^5 cell/cm^2 on all of the copolymer hydrogels [25].

In the case of HUVECs, the three stages of cell density change are also observed with an increase of the $|\zeta|$. When $|\zeta|$ ≤ 16.26 mV (F ≤ 0.3), no spreading cells are observed with an increase of the $|\zeta|$. This stage is denoted as non-proliferate stage. At this stage, the cells exhibit a round morphology and could not spread and proliferate on the copolymer hydrogels. When $|\zeta|$ = 20.83 mV (F = 0.4) ~ 22.18 mV (F = 0.5), the cell density obviously increases with an increase of the $|\zeta|$ (dramatically increase stage). At this stage, all of the cells spread extensively on the copolymer hydrogels, and the cells proliferate to form a confluent monolayer with a cell density of 1.03×10^5 cell/cm^2 and 1.25×10^5 cell/cm^2 when the $|\zeta|$ of copolymer hydrogels increases to 20.83 mV (F = 0.4) ~ 22.18 mV (F = 0.5), respectively. Furthermore, when $|\zeta|$≥ 22.18 mV (F ≥ 0.5), the cell density does not obviously change with an increase of the $|\zeta|$ of copolymer hydrogels (stable proliferation stage). At this stage, all of the cells proliferate to form a confluent monolayer with a cell density maintain at *ca.* 1.3×10^5 cell/cm^2 [25].

The above results demonstrate that there is a critical Zeta potential, $\zeta_{critical}$, of the poly(NaAMPS-*co*-DMAAm) hydrogels for controlling cell proliferation, $\zeta_{critical}$ = -20.83 mV (F = 0.4), below which the BFAECs and HUVECs are able to proliferate over the long term cultivation to form a confluent monolayer on the copolymer hydrogels.

The similar $\zeta_{critical}$ was also observed on the poly(NaSS-*co*-DMAAm) hydrogels with various $|\zeta|$. Figure 6 shows the typical phase-contrast micrographs of BFAECs after 6 h and 96 h cultivation on the poly(NaSS-*co*-DMAAm) hydrogels with various absolute values of Zeta potential, $|\zeta|$. The morphology of cells relates to the structures of actin fibers and focal adhesion. Vinculin is a membrane cytoskeleton protein found in focal adhesion plaques that is involved in

the linkage of integrin adhesion molecules to the actin cytoskeleton. Figure 7 shows actin stress fibers and focal adhesions, vinculin, of the BFAECs cultured on poly(NaSS-*co*-DMAAm) hydrogels with $|\zeta|$ = 9.4 mV (F = 0.06) and $|\zeta|$ = 20.5 mV (F = 0.5). It shows that the actin fibers and vinculin of the cultured BFAECs depend on the Zeta potential of the copolymer hydrogels. When $|\zeta|$ = 9.4 mV (F = 0.06), spreading cells are deficient in actin stress fibers and vinculin-containing complexes distributed only around the edge of the ECs. On the other hand, when $|\zeta|$ = 20.5 mV (F = 0.5), well-developed actin stress fibers and large vinculin-containing focal adhesion complexes are homogeneously distributed in the ECs. The structure of the actin stress fibers and focal adhesions indicate that the BFAECs are able to form stable focal adhesions on the copolymer hydrogels with high $|\zeta|$ value, i.e. high charge density, whereas the weak adhesion is formed on the hydrogels with low $|\zeta|$ value, i.e. low charge density [26].

Figure 8 shows the cell density of BFAECs at 96 h as a function of the $|\zeta|$ of the poly(NaSS-*co*-DMAAm) copolymer hydrogels. The same as BFAECs cultured on the poly(NaAMPS-*co*-DMAAm) copolymer hydrogels, there are three stages of cell density change with an increase of the $|\zeta|$ of the poly(NaSS-*co*-DMAAm) gels, i.e., slowly increase stage, dramatically increase stage, and stable proliferation stage. At slowly increase stage, $|\zeta| \leq 12.6$ mV (F ≤ 0.1), the BFAECs exhibit a round morphology or slight spreading with a few irregular protrusions at 6 h. However, the cells could not proliferate, and thus gradually died with the passage of culture time. The cell density decreases to 1.0×10^4 cell/cm^2 at 96 h which is even lower than the initial seeded cell density. At the dramatically increase stage, $|\zeta|$ = 14.0 mV (F = 0.2), all of the ECs spread extensively on the copolymer hydrogels. Furthermore, these spreading cells proliferate to form a confluent monolayer with a cell density of *ca.* 1.45×10^5 cell/cm^2 at 96 h. At the stable proliferation stage, $|\zeta| \geq 14$ mV (F ≥ 0.2), the cell density does not obviously change with an increase of $|\zeta|$, all of the ECs proliferate to form a confluent monolayer with a cell density saturates at *ca.* 1.5×10^5 cell/cm^2.

The above results demonstrate that the critical Zeta potential $\zeta_{critical}$ of the poly(NaSS-co-DMAAm) hydrogels exists at $\zeta_{critical}$=-14.0 mV (F = 0.2), below which the cells are able to initially spread and proliferate over the long term culture to form a confluent monolayer. This result shows that in the case of poly(NaSS-*co*-DMAAm) copolymer hydrogel, the critical zeta potential, $\zeta_{critical}$, shifts to a higher value of $\zeta_{critical}$=-14.0 mV for BFAEC proliferation, comparing with $\zeta_{critical}$=-20.83 mV of poly(NaAMPS-co-DMAAm) copolymer hydrogel. It is considered that PNaSS with aromatic ring close to the ionizable group facilitates protein adsorption from serum containing culture medium than that of PNaAMPS. The present results suggest that not only Zeta potential, but also chemical structure affects cell proliferation.

2.2.2 Effect of Zeta potential on dynamic cell behaviors

Cell motility plays an important role in a wide variety of biological processes such as embryogenesis, inflammatory response, wound healing, and the metastasis of tumor cells [27–31]. In particular, the migration of vascular ECs, which form the inner lining of blood vessels, is essential for angiogenesis [32,33]. As described in 3.2.1, Zeta potential (ζ) of the hydrogels affects the static behavior of ECs, such as cell morphology, proliferation, cytoskeleton structure and focal adhesion. Thus, effect of Zeta potential (ζ) on dynamic behavior of ECs, such as migration velocity, migration distance, and morphology oscillation were further investigated.

It has been reported that the migration velocity of cells is affected by the Young′s modulus (*E*) of the PAAm gel modified by collagen [34]. Therefore, for studying the effect of ζ on cell dynamic behaviors, designing hydrogels with various ζ, and at the same time, maintaining an identical *E* are necessary. As shown in Figure 9, a series of poly(NaSS-*co*-DMAAm) copolymer hydrogels, of which the $|\zeta|$ changes in the large range of 8.8 – 20.5 mV, and at the same time, the *E* changes in a small range of 160 – 198 kPa, could be synthesized by maintaining the total monomer (mixture of NaSS and DMAAm) concentration at 1M and crosslinker (MBAA) concentration at 4 mol%, while varying the molar fraction (F) of NaSS in the monomer mixture between 0.05 and 0.5. The study found that the migration velocity of the BFAECs decreases

with a increase in $|\zeta|$, and the cells exhibit an abrupt decrease in migration velocity at $\zeta_{critical}$ = -14.0 mV.

Figure 10 shows the spreading area and the average migration velocity of the BFAECs cultured for 6 to 12 h as a function of the $|\zeta|$ of poly(NaSS-*co*-DMAAm) copolymer hydrogels. When 8.8 mV $<|\zeta|<$ 12.6 mV (F = 0.05 – 0.1), the spreading area of EC is *ca.*1000 μm^2, and the average migration velocity of the ECs is *ca.* 1.5 μm/min. Whereas, when $|\zeta|$ = 14.0 mV (F = 0.2), the spreading area of EC is dramatically increases to 1496 μm^2, and the average migration velocity of the ECs dramatically decreases to 0.97μm/min. Furthermore, when $|\zeta|$ = 20.5 mV (F = 0.5), the spreading area of ECs is dramatically increases to 2028 μm^2, and the average migration velocity of the ECs dramatically decreases to 0.73 μm/min. Considering the relationship between the cell area and the ζ, we can find that the migration velocity of the ECs is related to their shape: an extensively spreading cell migrate slowly and vice versa. The present study demonstrated that not only the elasticity but also the charge density of the hydrogel affects the area and migration velocity of cultured cells.

It is interesting to note that when 8.8 mV $<|\zeta|<$ 12.6 mV (F = 0.05–0.1), the BFAECs do not proliferate and shows high migration velocity. In fact, the cease of proliferation of ECs can be observed in the process of new blood vessels formation *in vivo*. The formation of new blood vessels is a multistep process in which the activated ECs of existing vessels degrade the underlying basement membrane, migrate, and proliferate in the perivascular stroma to form capillary sprouts. These sprouting ECs cease proliferation, align, form tubes with a patent lumen, and deposit a basement membrane to finally yield new operational blood vessels [34]. Therefore, studying on the motility of ECs that is not able to proliferate could reveal some information on angiogenesis.

We have found that an individual BFAEC repeatedly changes its morphology when 8.8 mV $<|\zeta|<$ 12.6 mV (F = 0.05–0.1). In this morphology oscillation process, a spreading cell shrink its extended morphology to a round shape only in the time less than 1 min, whereas a round shape cell changes its morphology to an extensively spreading cell need *ca.* 20 min (Figure 11a).

The large time difference between cell spreading and shrinkage implies that the polymerization of actin fibers take a longer time than their depolymerization.

Figure 11b shows a typical example of a BFAECs with its morphology oscillating from a spread shape to a round shape when $|\zeta|$ = 9.4 mV (F = 0.06). The filopodia of an extensively spreading cell shrank (Figure 11b-2), indicating that the EC was released from the pre-existing sites of adhesion. As a result, the EC rapidly changed to a round shape and migrated to another location (Figure 11b-3). This process was very fast and was completed within 1 min. The round EC subsequently remained at its new location for *ca.* 10 min (Figure 11b-11), lamellipodia then began to develop after 11 min (Figure 11b-12), and pseudopodia gradually grew with the passage of culture time. The filopodia of the EC could be obviously observed at 15 min (Figure 11b-16). As a result, the EC changed back to an extensively spreading shape after 20 min (Figure 11b-21). The lamellipodia and filopodia then grew continuously until 30 min (Figure 11b-32) [26].

It is well known that a spreading cell gradually reverts to a round shape in order to undergo mitosis. In the present study, however, the cells cultured on the hydrogels which 8.8 mV < $|\zeta|$ < 12.6 mV (F = 0.05–0.1) are not able to divide during the process of morphological change, indicating that the change in cell morphology is not associate with mitosis.

It has been reported that fibronectin affects certain cell behaviors, such as the rate and anisotropism of spread, traction force (the forces exerted by cells on its scaffold during spreading), and cell-scaffold adhesive force, as well as migration velocity [35,36]. Our study further found that fibronectin affects EC oscillation on the hydrogels with low charge density in a stick–slip mode.

2.2.3 Correlation between fibronectin adsorption and cell behaviors

The above results demonstrated that the ζ of the hydrogels has a profound effect on the static behaviors and dynamic behaviors of the ECs. It is a question why the EC behaviors can be affected by the ζ of synthetic hydrogels. Because the hydrogels that enhance cell proliferation are negatively charged, and the cell surface is negatively charged also, therefore, there is no direct electrostatic interaction between the hydrogel and the cultured ECs. We assumed that proteins contained in the FBS could adsorb on the hydrogel surface and act as bridges between

cultured ECs and hydrogels, which affect static and dynamic behavior of the ECs. In other word, if ζ affects the amount of adsorbed proteins on the hydrogels, it should affect the behaviors of ECs. Thus, the correlation between adsorption total amount of protein and a typical cell-adhesive protein, fibronectin, from cell cultured medium on the hydrogel surface and cell behavior are furthermore analyzed.

The same as the relationship between the cell density and the absolute value of Zeta potential, $|\zeta|$, the concentration of total adsorbed proteins (C_p) and fluorescence intensity of fibronectin (F_f) change with an increase of the $|\zeta|$ of the poly(NaAMPS-*co*-DMAAm) copolymer hydrogels could also be divided into three stages, i.e., slowly adsorbed stage, dramatically adsorbed stage and stable adsorption stage (Figure 12).

At slowly increase stage, $|\zeta|$ ≤ 16.26 mV (F ≤ 0.3), the value of C_p and F_f is *c.a.* 9 μg/cm^2 and 1.0×10^6 *a.u.*, respectively, and both of the values slowly increases with an increase of the $|\zeta|$. At dramatically adsorbed stage, $|\zeta|$ = 20.83 mV (F = 0.4), the value of C_p and F_f extensively increases to *c.a.* 11.5 μg/cm^2 and 6.0×10^6 *a.u.*, respectively. At stable adsorption stage, $|\zeta|$ > 20.83 mV (F > 0.4), the value of C_p and F_f maintains at a stable high value, which nearly not change with an increase of the $|\zeta|$. The effects of the $|\zeta|$ on total proteins adsorption and fibronectin adsorption coincide well with cell behaviors (Figure 8). The results indicates that the charge density of hydrogels adjusts protein adsorption, that is, more negative charge, more protein adsorption, which favors cell proliferation, and the migration velocity of the cells is low, on the other hand, a little negative charge, a little protein adsorption, which not suitable cell proliferation, and the migration velocity of the cells is high.

Effect of protein adsorption on cytoskeleton and focal adhesions could clearly visualize actin stress fibers and focal adhesions (Figure 7). When $|\zeta|$ = 9.4 mV, only a little protein adsorption, the spreading ECs deficient in actin stress fibers and focal adhesions, implying that the ECs are unable to form stable focal adhesions on the hydrogel. Consequently, the ECs undergo a dramatic oscillation in shape factor. On the other hand, when $|\zeta|$ = 20.5 mV, more protein adsorption, the spreading ECs has well-developed actin fibers and large focal adhesions,

implying that the ECs are able to form stable focal adhesions on the hydrogel. Such ECs thus maintain a stable spreading shape factor.

2.3 *Effect of hydrogel properties on EC function*

The major problem of the artificial blood vessel is that blood clot occurs after a certain period of implantation, especially when the diameter of artificial blood vessel is smaller than 5mm [37]. The ideal artificial blood vessel should have the structure similar to *in vivo* blood vessel and take full advantages of cell functions. Therefore, hybrid artificial blood vessel with EC monolayer on its inner wall has been expected to inhibit thrombosis. Our investigation demonstrates that the platelet adhesion on the two kinds of human ECs, i.e., HUVECs and HCAEC, strongly dependents on the chemical structure and Young's modulus of synthetic hydrogels. Furthermore, the different platelet adhesion behaviors are attributed to the amount of glycocalyx secreted by the ECs cultured on different kinds of hydrogel scaffolds. The ECs cultured on the PNaSS hydrogel secrets more glycocalyx which contributes to inhibit platelet adhesion. The results imply that it is possible to fabricate hybrid artificial blood vessel with high blood compatibility from PNaSS hydrogel with ECs monolayer on its inner surfaces.

2.3.1 *Effect of chemical structure on platelet adhesion*

HUVECs could proliferate to sub-confluent (PAA *M* =1, 2 mol%) or confluent on negatively charged hydrogels (PNaAMPS *M* =2, 10 mol%, PNaSS *M* =4, 10 mol%) which is not sensitive to the *M* of the hydrogels. Figure 13 shows the typical phase-contrast micrographs of the HUVECs cultured on the various kinds of hydrogels at 144 h (Column I), and the SEM images of the adhered platelets on the correspond HUVECs (Column II). After cultured for 144 h, HUVECs proliferate to confluent on the strong negatively charged hydrogels, PNaAMPS (*M*=2, 10mol%) and PNaSS (*M*= 4, 10mol%), with a cell density *c.a.* 1.2×10^5 cell/cm^2, closed to that on the TCPS plate. On the other hand, HUVECs proliferated to subconfluent on the weak negatively charged PAA (*M* = 1, 2 mol%) hydrogel with a cell density of *c.a.* 4.5×10^4 cell/cm^2. The results demonstrates that same as BFAECs, HUVECs proliferation dependents on the chemical structure of hydrogels. Platelet compatibility of the cultured HUVECs was analyzed by static platelet adhesion test.

As revealed by human platelet adhesion test in static conditions, the behavior of platelet adhesion on HUVEC surface obviously dependents on the chemical structure of the hydrogel

scaffolds. In the case of weak negatively charge PAA hydrogel, the density of adhered platelets (D_p) is not dependent on the *M* of the hydrogels, and D_p = 115×10^4 platelet/μm^2 on the subconfluent HUVECs. In the case of strong negatively charge hydrogel, PNaAMPS, the D_p of the cultured HUVEC monolayer decreases with an increase of the *M*. When *M* = 2, 10mol%, D_p = 183, 6 ×10^4 platelet/μm^2, respectively. In the case of another strong negatively charge hydrogel, PNaSS, it is a surprising result that no platelets adhere on the HUVEC monolayers cultured on the PNaSS gels, regardless of the *M* of the hydrogels [38]. The above results demonstrate that the anti-platelet adhesion of the HUVECs cultured on various hydrogel scaffolds increases in the order of PNaSS <PNaAMPS< PAA.

2.3.2 Effect of Young's modulus on platelet adhesion

It was reported that heparan sulfate proteoglycans (HSPGs), which is a main component of proteoglycans contained in glycocalyx, exhibit antithrombin activity [39,40]. Combining with the above described results, we hypothesized that the glycocalyx secreted the ECs can be affected by the physic-chemical properties of the hydrogel scaffolds because platelet adhesion closely correlates to the glycocalyx. To verify this, the correlation between the platelet adhesion and the amount of glycocalyx of ECs cultured on the PNaSS hydrogels with various levels of Young's modulus (*E*) rang in 3 ~ 263 kPa was further studied.

Same as HUVECs, HCAECs could proliferate to confluence on the PNaSS hydrogels with various *E*. In addition, real-time polymerase chain reaction (PCR) and glycosaminoglycan assay showed that the amount of EC-specific glycocalyx, glypican, syndecan-4, and perlecan, secreted by the cultured HCAECs increases with an increase of the *E* of PNaSS hydrogel, which obviously higher than that cultured on TCPS. Furthermore, the HCAECs cultured on PNaSS hydrogels showed excellent property against platelet adhesion. The largest amount of EC-specific glycocalyx and excellent blood compatibility were observed when *E* > 60 kPa.

Figure 14 shows the morphology of HCAECs cultured for 120 h on PNaSS hydrogels with *E* = 3, 60, 100 kPa, corresponding *M* =4, 10, 13 mol%. The HCAECs could proliferate to confluence at 120 h on the PNaSS hydrogels with cell density of *c.a.*1.25×10^5 cell/cm^2, and the proliferation behavior dose not dependent on the *E*. However, the morphology of the cells changes with an increase of *E*. When *E* = 3, 17, 40 kPa, the HCAECs perform round shape or polygonal which is

similar on the ECs cultured on the TCPS with E = 3 GPa. When E = 60 kPa, *c.a.* 40% the ECs perform fusiform or spindle, and the number of fusiform or spindle cells increases with an increase of E. When E = 263 kPa, all HCAECs shows spindlical morphology. The results demonstrate that the elasticity of cell scaffold has a remarkable influence on the morphology of HCAECs, the ECs show round morphology when the cells cultured on the very soft (E < 40 kPa) or very hard (~ GPa) scaffolds, but elliptic on the hydrogels with intermediate elasticity (40 kPa <E < 263 kPa). Furthermore, the cell morphology is more homogenous on the hydrogel scaffolds than that on TCPS [41].

HSPGs of ECs consist of a core protein and heparan sulfate-type glycosaminoglycans (GAGs). There are five distinct HSPG core proteins in ECs: syndecan-1, syndecan-2, syndecan-4, glypican and prelecan. It was reported that prelecan exhibit antithrombin activity by activing antithrombin III though heparin-like sequences in the heparin sulfate chains [42]. For investigating the effect of the Young's modulus (E) of hydrogel on the amount of glycocalyx secreted by HCAECs, the relative RNA levels of core proteins and the amount of GAG were analyzed.

The relative RNA expressions of the specific core proteins in glycocalyx, glypican, syndecan-4, and perlecan, and the relative amount of total GAG, are also shown in Figure 14. The results demonstrate that HCAECs cultured on hydrogels secret a larger amount of glycocalyx than those cultured on TCPS scaffold. Furthermore, the amount of glycocalyx is influenced by the elasticity of the PNaSS hydrogel scaffolds, harder PNaSS hydrgels promote the secretion of glycocalyx.

The density of platelets that adhered on the HCAEC monolayer cultured on PNaSS hydrogels decreases with an increase of E. The density of platelets that adhered to the HCAEC monolayer cultured on the PNaSS hydrogels with E = 60, 100 kPa is 1.2×10^5 platelets/μm^2 and 3×10^4 platelets/μm^2, respectively, which is *c.a.* 8 and 30 times lower than that on the PNaSS hydrogel with E = 3 kPa. The result is consistent with the result of the relative RNA levels of glypican, syndecan-4, and perlecan, as well as the amount of GAG assay described above.

The results suggested that the glycocalyx of cultured ECs modulates platelet compatibility, and the amount of glycocalyx secreted by ECs dependents on the chemical structure and Young's modulus (E) of hydrogel scaffolds. This result should be applied to make the hybrid artificial

blood vessel composes of hydrogels and ECs with high platelet compatibility.

3 . Conclusions

We have found that some negatively charged synthetic hydrogels, such as PNaAMPS and PNaSS, can directly promote cell proliferation, with no need of surface modification by any cell-adhesive proteins or peptides at the environment of serum-containing medium. The main conclusions are as following:

(1) Effect of chemical structure on cell proliferation. Synthetic hydrogels facilitate ECs proliferation decreases in the order of negatively charged strong polyelectrolyte gels (PNaAMPS, PNaSS) > negatively charged weak polyelectrolyte gels (PAA, PMAA) > neutral gels (PVA, PAAm, PDMAAm).

(2) Effect of Zeta potential (ζ) on cell behaviors. (i) Critical Zeta potential for EC proliferation is $\zeta_{critical} = -20.83$ mV and $\zeta_{critical} = -14.0$ mV for poly(NaAMPS-*co*-DMAAm) and poly(NaSS-*co*-DMAAm), respectively. (ii) When $\zeta > \zeta_{critical}$ the ECs exhibited a small spreading area, fast migration velocity and oscillation in a stick–slip mode from a spreading morphology to round shape, with concurrent deficiency in actin fibers and less prominent focal adhesions. Conversely, when $\zeta \leq \zeta_{critical}$, the ECs exhibited a large spreading area, slow migration velocity and stable spreading morphology, with concurrent well-developed actin fibers and prominent focal adhesions. Furthermore, the cell behavior is well correlated with the adsorption of all the amount of proteins and fibronectin contained in cell culture medium on the hydrogel surfaces.

(3) Effect of chemical structure and Young's modulus on EC function. The anti-platelet adhesion of the ECs cultured on various hydrogel scaffolds increases in the order of PNaSS <PNaAMPS< PAA. Furthermore, adhered platelets on the ECs cultured on the hydrogel scaffolds obviously decreases with an increase of the Young's modulus (E) of the hydrogels, especially when E > 60 kPa. In addition, the anti-platelets adhesion is well correlate with the EC-specific glycocalyx. It implied that the hydrogels with high elasticity enhances ECs to secret more glycocalyx which contributes to the inhibition of platelet adhesion

The above new finding that the synthetic hydrogel scaffolds can manipulates static and dynamic

behaviors of cells and are suitable for cells to maintain their original functions will open a new era of soft and wet materials used in basic study and biomedical application in tissue engineering.

Acknowledgements

YM Chen thanks Zhen Li, Kun Dong, Zhen Qi Liu for their help in manuscript preparation.

References

1 Bao, G., Suresh, S., Nat. Mater., 2003, 2:715–725

2 Discher, D. E., Janmey, P., Wang, Y. L., Science, 2005, 310:1139–1143

3 Wakatsuki, T., Kolodney, M. S., Zahalak, G. I., Elson, E. L., Biophys. J., 2000, 79:2353–2368.

4 Belmadani, S., Zerfaoui M., Boulares H.A., Palen D.I., Matrougui K., Am. J. Physiol. Heart Circ. Physiol. 2008, 295:H69-76

5 Lua, J. T., Lee, C.J., Bent, S. F., Fishman, H.A., Sabelman, E.E., Biomaterials,2007,28: 1486–1494

6 Firel, R., Sar, S., Mee, P.J., Adv Drug Deliv Rev, 2005, 57(13):1894-1903

7 Hwang, N.S., Varghese, S., Elisseeff, J. , Adv. Drug Del. Rev. ,2008, 60:199–214

8 West, J.L., Hubbell, J.A., Macromolecules, 1999,32:241–244

9 Schmedlen, R.H., Masters, K.S., West, J.L. , Biomaterials, 2002,23:4325–4332

10 Wang Y.L., Janmey P., Discher D.E., Science, 2005,310:1139–1143

11 Lo, C. M., Wang, H. B., Dembo, M. and Wang, Y. L., Biophys. J., 2000,79:144–152

12 Haga, H., Irahara, C., Kobayashi, R., Nakagaki, T., Kawabata, K., Biophys. J., 2005, 88:2250–2256

13 Beningo, K. A., Lo, C. M., Wang, Y. L., Methods. Cell Biol., 2002,69:325–339

14 Peyton, S. R., Putnum, A., J. Cell Physiol., 2005, 204:198–209

15 Yeung, T., Georges, P. C., Flanagan, L. A., Marg, B., Ortiz, M., Funaki, M., Zahir, N., Ming, W., Weaver, V. and Janmey,P. A., Cell Motility Cytoskeleton, 2005, 60:24–34

16 Pelham, R. J. Jr and Wang, Y. L., Proc. Natl. Acad. Sci. USA., 1997, 94:13661–13665

17 Chen, Y. M., Shiraishi, N., Satokawa, H., Kakugo, A., Narita, T., Gong, J.P., Osada, Y.,

Yamamoto, K., Ando, J., Biomaterials, 2005, 26:4588–4596

18 Lamalice, L., Boeuf, F. L. and Huot, J., Circ. Res., 2007, 100, 782–794

19 Davis, G. E. and Senger, D. R., Circ. Res., 2005, 97, 1093–1107

20 Pries, A.R., Secomb, T.W., Jacobs, H., Am. J. Physiol., 1997, 273:H2272–H2279

21Vink, H., Constantinescu, A.A., Spaan, J.A.E., Circulation , 2000, 101:1500–1502

22 Weitz, J.I., J. Clin. Invest. 2003,111:952–954

23 Tanaka, Y.; Kuwabara, R., Na, Y.H., Kurokawa, T., Gong, J.P., Osada, Y., Phys. Chem. B, 2005, 109(23):11559-11562

24 Chen, Y. M., Gong, J. P., Yasuda, Y., "Gel: a potential material as artificial soft tissue, in: Macromolecular Engineering: Precise Synthesis, Materials Properties, Applications, Vol. 4",ed. by K. Matyjaszewski,Y. Gnanou and L. Leibler, WILEY-VCH, Weinham, 2006,pp. 2689–2718

25 Chen, Y.M., Gong, J.P., Tanaka, M., Yasuda, K., Yamamoto, S., Shimomura, M., Osada, Y., J. Biomed. Mater. Res., 2009, 88A: 74–83

26 Chen, Y.M., Ogawa, R., Kakugo, A., Osada, Y., Gong, J.P., Soft Matter, 2009, 5:1804–1811

27 Bronner-Fraster, M., Trends Cell Biol., 1993, 3:392–397

28 Singer, S. J. and Kupfer, A., Ann. Rev. Cell Biol., 1986, 2:337–365

29 Hauzenberger, D., Klominek, J., Holgerson, J., Bergstrom, S. E. and Sundqvist, K. G., Immunol, J., 1997,158:76–84

30 McCrawley, L. J., O'Brian, P. and Hudson, L. G., Endocrinology, 1997, 138:121–127

31 Van Roy, F. and Mareel, M., Trends Cell Biol., 1992, 2:163–169

32 Lamalice, L., Boeuf, F. L. and Huot, J., Circ. Res., 2007, 100:782–794

33 Davis, G. E. and Senger, D. R., Circ. Res., 2005, 97:1093–1107

34 Lo, C. M., Wang, H. B., Dembo, M. and Wang, Y. L., Biophys. J., 2000, 79, 144–152

35 Deroanne, C.F., Lapiere, C.M., Nusgens, B.V., Cardiovasc Res., 2001,49:647-658

36 Palecek, S.P., Loftus, J.C., Ginsberg, M.H., Lauffenburger, D.A., Horwitz, A.F., Nature, 1997,385:537– 540

37 Reinhart-King, C.A., Dembo, M. and Hammer, D.A. , Biophysical Journal, 2005,89(1): 676-689

38 Foley, D.P., Melkert, R., Serruys, P.W. , Circulation, 1994,90(3):1239–1251

39 Chen, Y.M., Tanaka, M., Gong, J. P., Yasuda, Y., Yamamoto, S.,Shimomura , M., Osada, Y., Biomaterials, 2007, 28: 1752–1760

40 Yanagishita, M., Hascall, V.C. , J. Biol. Chem., 1992,267:9451–9454

41 Yang, J.J., Chen, Y.M., Kurokawa, T., Gong, J.P., Onodera, S., Yasuda, K., J. Biomed. Mater. Res. A. ,2010 ,Aug 2. [Epub ahead of print] PMID: 20681030

42 Segev, A., Nili, N., Strauss, B.H., Cardiovasc. Res., 2004,63:603–610

Figure captions

Figure 1 Molecular structures of hydrogels (column III), i.e., neutral PAAm, PDMAAm and PVA, weak negatively charged PAA and PMAA, as well as weak negatively charged PNaAMPS and PNaSS, and typical phase-contrast micrographs of bovine fetal aorta endothelial cells (BFAECs) cultured on the hydrogels with various cross-linker concentrations (*M*) at 120 h (column V). PAAm (2 mol%), PDMAAm (4 mol%), PVA (6 mol%), PAA (2 mol%), PMAA (1 mol%), PNaAMPS (6 mol%), and PNaSS (10 mol%). Original magnification: × 10. Scale bar: 200μm. Revised with permission from the literature [17]

Figure 2 BFAEC proliferation kinetics on the surface of various hydrogel scaffolds. (◖) PVA (6 mol%), (♦) PAAm (4 mol%), (□) PAA (2 mol%), (○) PMAA (1 mol%), (Δ) PNaSS (10 mol%), (■) PNaMPS (6 mol%) and (▲) Collagen gel as a control. Error ranges are standard deviations over n = 4~8 samples. Revised with permission from the literature [17]

Figure 3 The molar fraction, F, as a function of absolute value of zeta potential, $|\zeta|$, of HEPES buffer-equilibrated poly(NaAMPS-*co*-DMAAm) hydrogels. Revised with permission from the literature [25]

Figure 4 Cell density at 120 h as a function of absolute value of Zeta potential, $|\zeta|$, of poly(NaAMPS-*co*-DMAAm) hydrogels. (●) BF AECs (○) HUVECs. Error ranges are standard deviations over n = 4~8 samples. Revised with permission from the literature [25].

Figure 5 Phase-contrast micrographs of BFAECs (column I) and HUVECs (column II) cultured on poly(NaAMPS-*co*-DMAAm) hydrogels with various molar fraction, F, corresponding to various absolute value of Zeta potential, $|\zeta|$. Cultivation time: 120 h. Scale

bar: 200 μm. Revised with permission from the literature [25].

Figure 6 Phase-contrast micrographs of BFAECs cultured on poly(NaSS-*co*-DMAAm) gels with absolute value of Zeta potential, $|\zeta|$, at 6 h and 96 h. Scale bar: 50 μm. Revised with permission from the literature [26].

Figure 7 Actin stress fibers and focal adhesions, vinculin, of the cells cultured on poly(NaSS-*co*-DMAAm) gels with $|\zeta|$ = 9.4 mV (F = 0.06) and $|\zeta|$ = 20.5 mV (F = 0.5). Scale bar: 20 μm. Reproduced with permission from the literature [26].

Figure 8 The cell density on poly(NaSS-*co*-DMAAm) gels at 96 h as a function of the absolute value of Zeta potential, $|\zeta|$. Error ranges are the standard deviations over n = 3~6 samples. Revised with permission from the literature [26].

Figure 9 The absolute value of Zeta potential ($|\zeta|$) (○) and Young's modulus (E) (●) of poly(NaSS-co-DMAAm) gels as a function of molar ratio (F = 0.05~0.5). Error range for ζ is the standard deviations over n = 70~100 gel particles; error ranges for E is the standard deviations over n = 4~6 samples. Revised with permission from the literature [26].

Figure 10 The spreading area and the average migration velocity of the BFAECs cultured for 6 to 12 h as a function of the $|\zeta|$ of poly(NaSS-*co*-DMAAm) copolymer hydrogels. Revised with permission from the literature [26].

Figure 11a The morphological parameter (1-S) of the BFAECs cultured on poly(NaSS-co-DMAAm) hydrogels as a function of culture time. A round shape corresponds to 1-S→0, and a spreading shape corresponds to 1-S→1. (○) $|\zeta|$ = 9.4 mV (F =0.06), (●) $|\zeta|$ =20.5 mV (F=0.5). Reproduced with permission from the literature [26].

Figure 11b A typical example of morphology change of a BFAEC cultured on a poly(NaSS-co-DMAAm) hydrogel of $|\zeta|$ = 9.4 mV at 8.8–9.3 h recorded by CCD camera. The arrows show a BFAEC repeatedly changing from a spreading morphology to a round shape, and then changing back to spreading morphology with time. Time interval between successive images: 1 min. Reproduced with permission from the literature [26].

Figure 12 Concentration of total adsorbed proteins (◖) and fluorescence intensity of adsorbed fibronectin (■) on poly(NaAMPS-co-DMAAm) copolymer gels as a function of absolute value

of Zeta potential. Error ranges are standard deviations over n = 3~6 samples. Revised with permission from the literature [25].

Figure 13 The typical phase-contrast micrographs of the HUVECs cultured on the various kinds of hydrogels at 144 h (Column I), as well as the SEM images (Column II) and the density of adhered platelets (D_p) on the corresponding HUVECs. Revised with permission from the literature [39].

Figure 14 The typical phase-contrast micrographs of HCAECs cultured for 120 h on PNaSS hydrogels with E = 3, 60, 100 kPa, corresponding M =4, 10, 13 mol%, as well as the relative RNA expressions of the specific core proteins in glycocalyx, glypican, syndecan-4, and perlecan, the relative amount of total GAG. TCPS was used as a control. Revised with permission from the literature [41].

Column Ⅰ	Column Ⅱ	Column Ⅲ	Column IV	Column V
Charge	Hydrogel	Chemical structure	*M* (mol%)	BFAECs
Neutral charge	PAAm	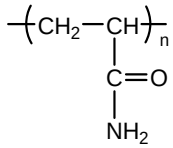	2	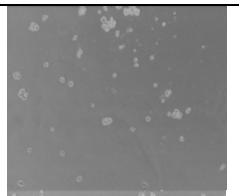
	PDMAAm	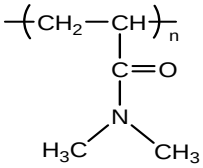	4	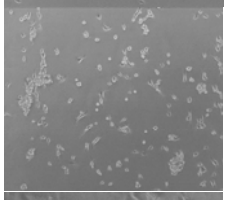
	PVA	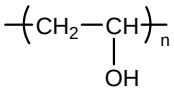	6	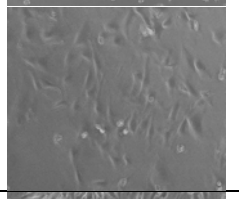
Weak negative charge	PAA	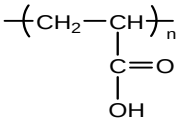	2	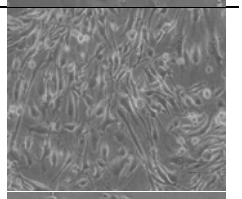
	PMAA	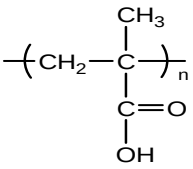	1	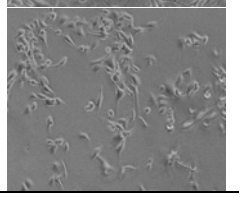
Strong negative charge	PNaAMPS	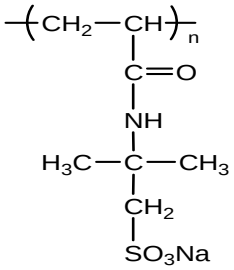	6	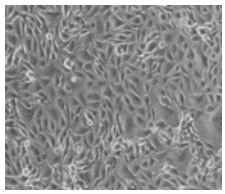
	PNaSS	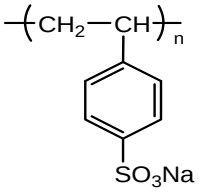	10	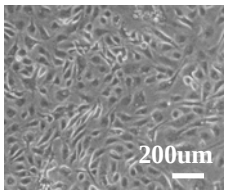

Figure 1

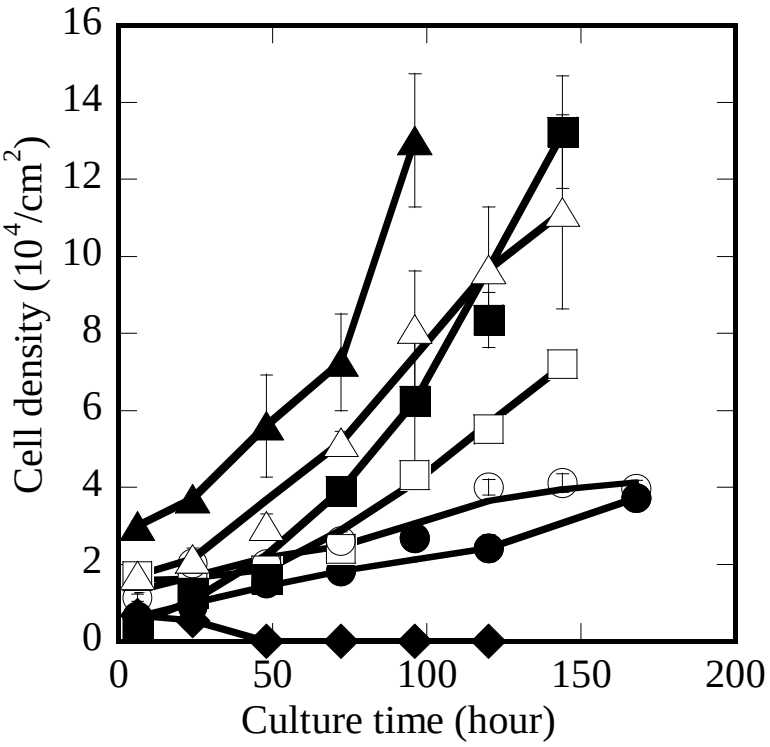
16
14
12
10
8
6
4
2
0
Cell density (10^4/cm^2)
0
50
100
150
200
Culture time (hour)

Figure 2

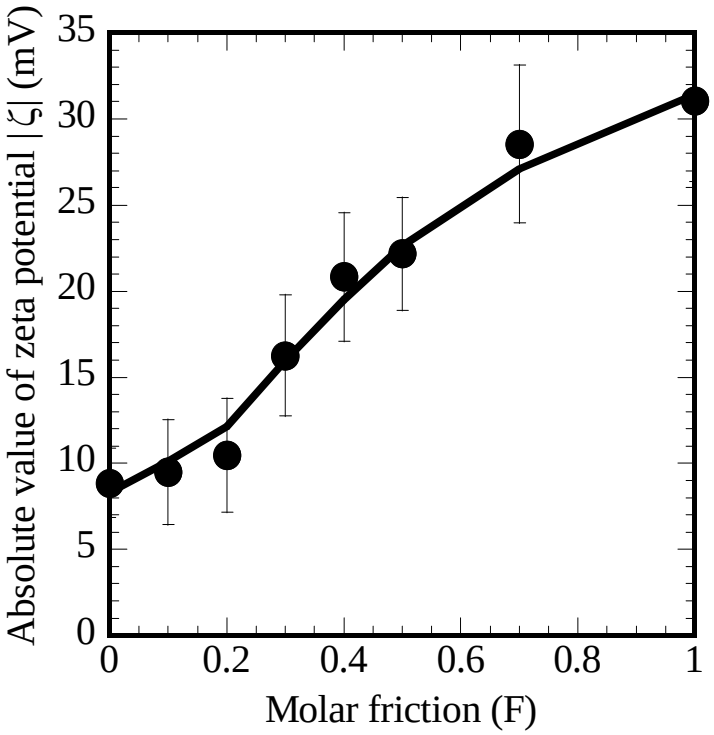
Absolute value of zeta potential |ζ| (mV)
35
30
25
20
15
10
5
0
0
0.2
0.4
0.6
0.8
1
Molar friction (F)

Figure 3

F	$\lvert\zeta\rvert$ (mV)	Column I	Column II
		BFAEC	HUVEC
0	8.65	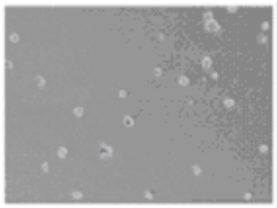	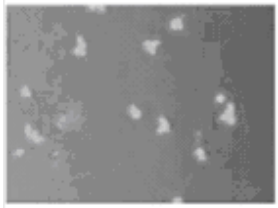
0.3	16.26	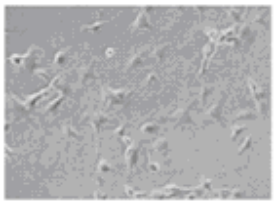	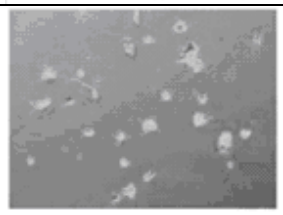
0.4	20.83	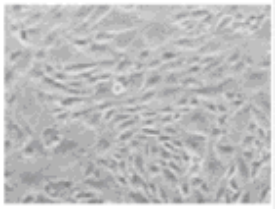	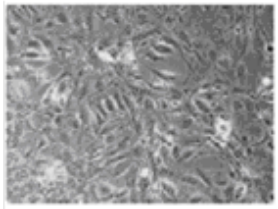
0.5	22.18	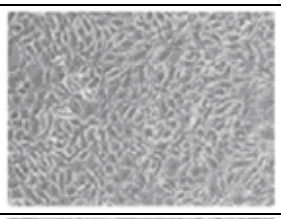	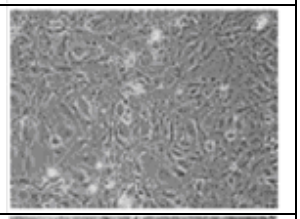
0.7	22.55	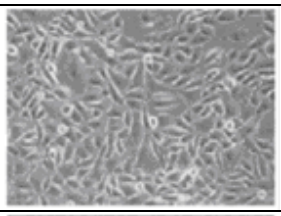	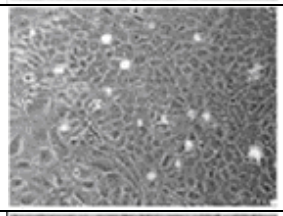
1.0	31.08	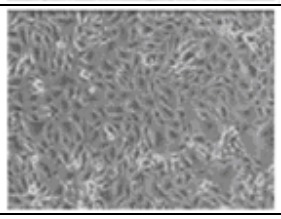	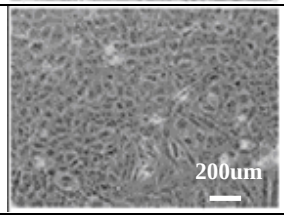

Figure 4

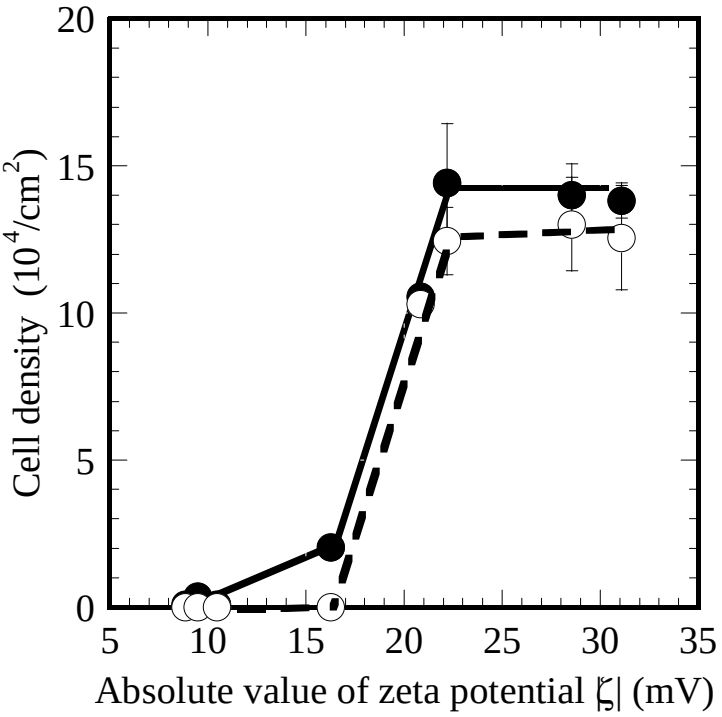
20
15
10
5
0
Cell density (10^4/cm^2)
5
10
15
20
25
30
35
Absolute value of zeta potential |ζ| (mV)

Figure 5

F	$\lvert\zeta\rvert$ (mV)	Column I	Column II
		6 h	120 h
0.05	8.8	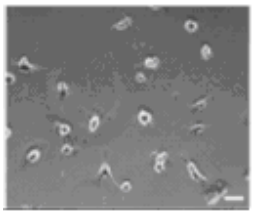	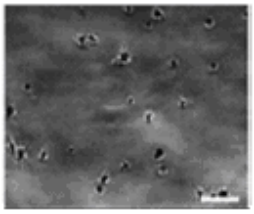
0.06	9.4	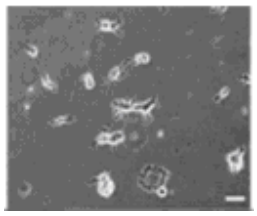	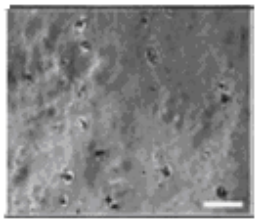
0.075	10.5	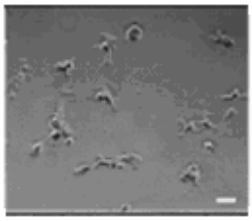	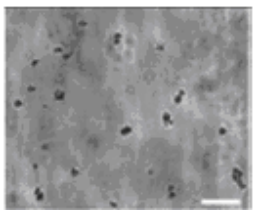
0.1	12.6	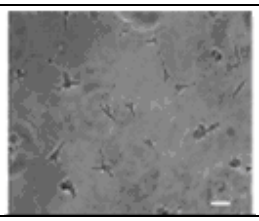	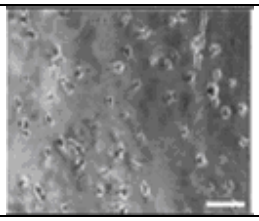
0.2	14.0	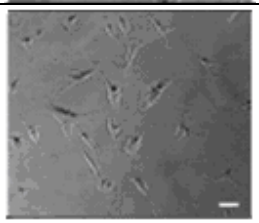	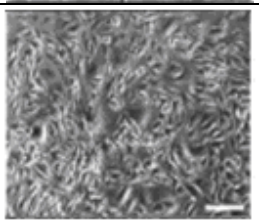
0.5	20.5	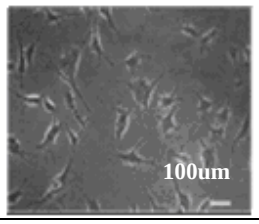	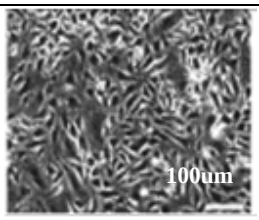

Figure 6

F	$\lvert\zeta\rvert$ (mV)	Stress fiber	Vinculin	Merge
0.06	9.4	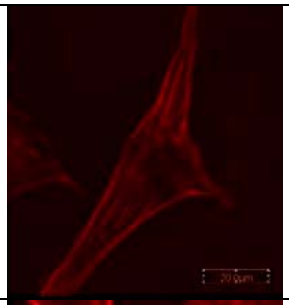	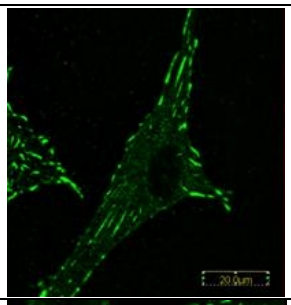	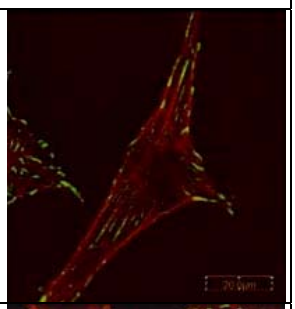
0.5	20.5	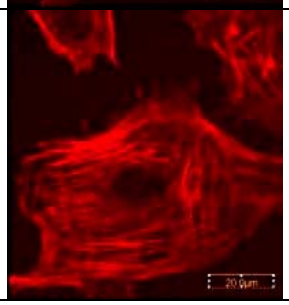	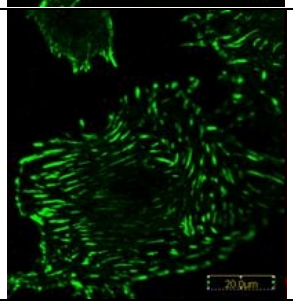	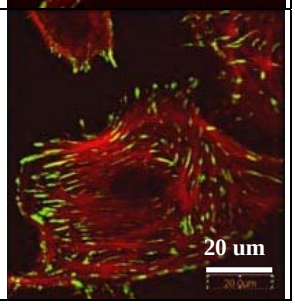

Figure 7

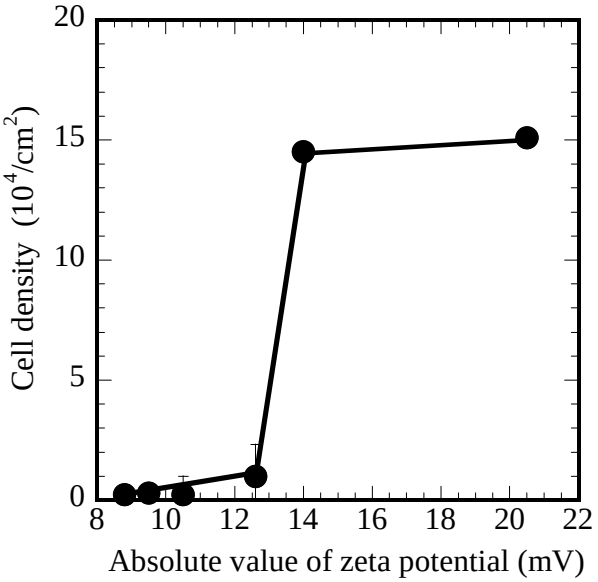
20
15
10
5
0
8
10
12
14
16
18
20
22
Cell density (10^4/cm^2)
Absolute value of zeta potential (mV)

Figure 8

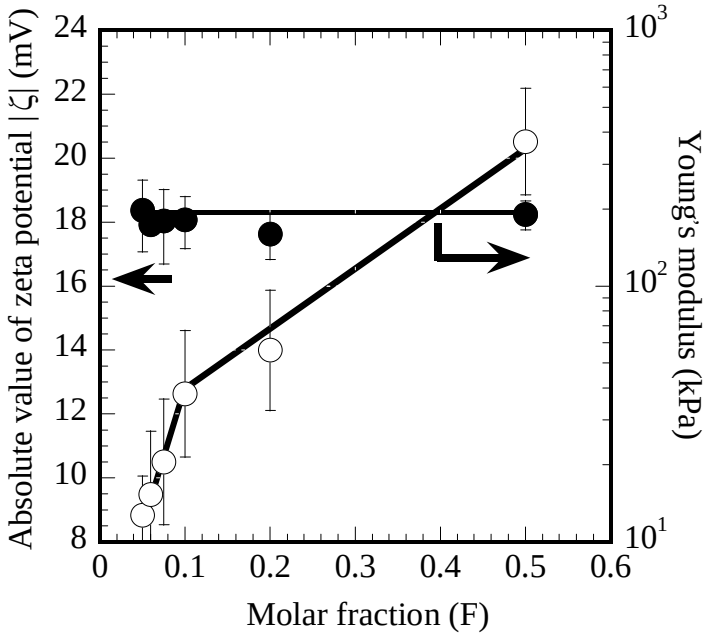
Absolute value of zeta potential |ζ| (mV)
Young's modulus (kPa)
Molar fraction (F)
24
22
20
18
16
14
12
10
8
0
0.1
0.2
0.3
0.4
0.5
0.6
10^3
10^2
10^1

Figure 9

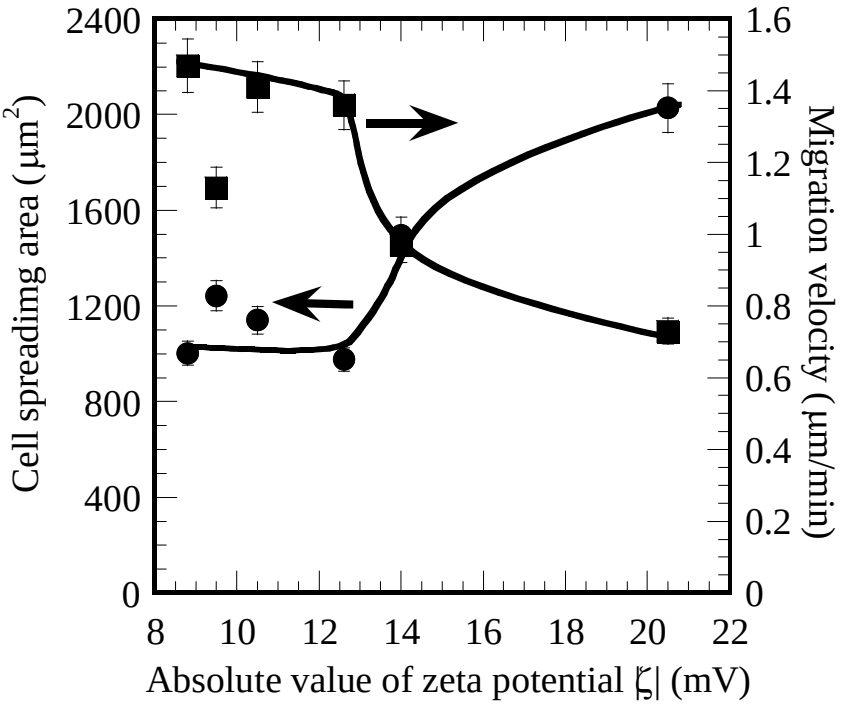
2400
2000
1600
1200
800
400
0
Cell spreadimg area (μm2)
1.6
1.4
1.2
1
0.8
0.6
0.4
0.2
0
Migration velocity (μm/min)
8
10
12
14
16
18
20
22
Absolute value of zeta potential ζ| (mV)

Figure 10

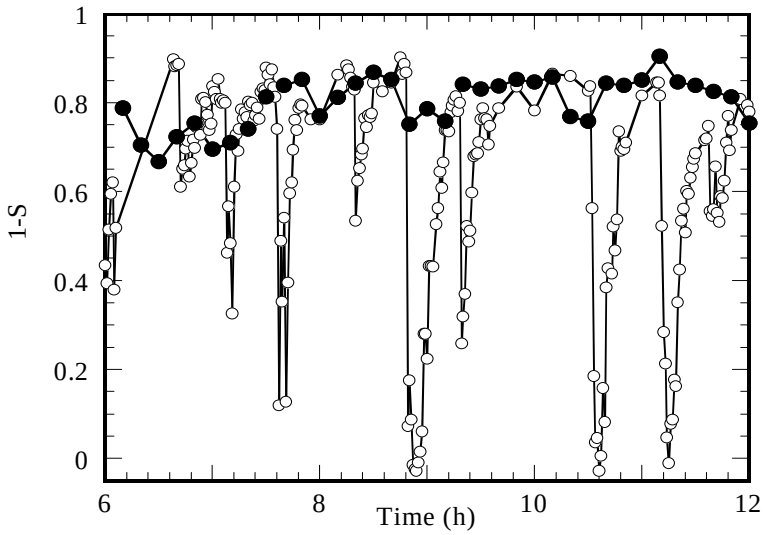

Figure 11a

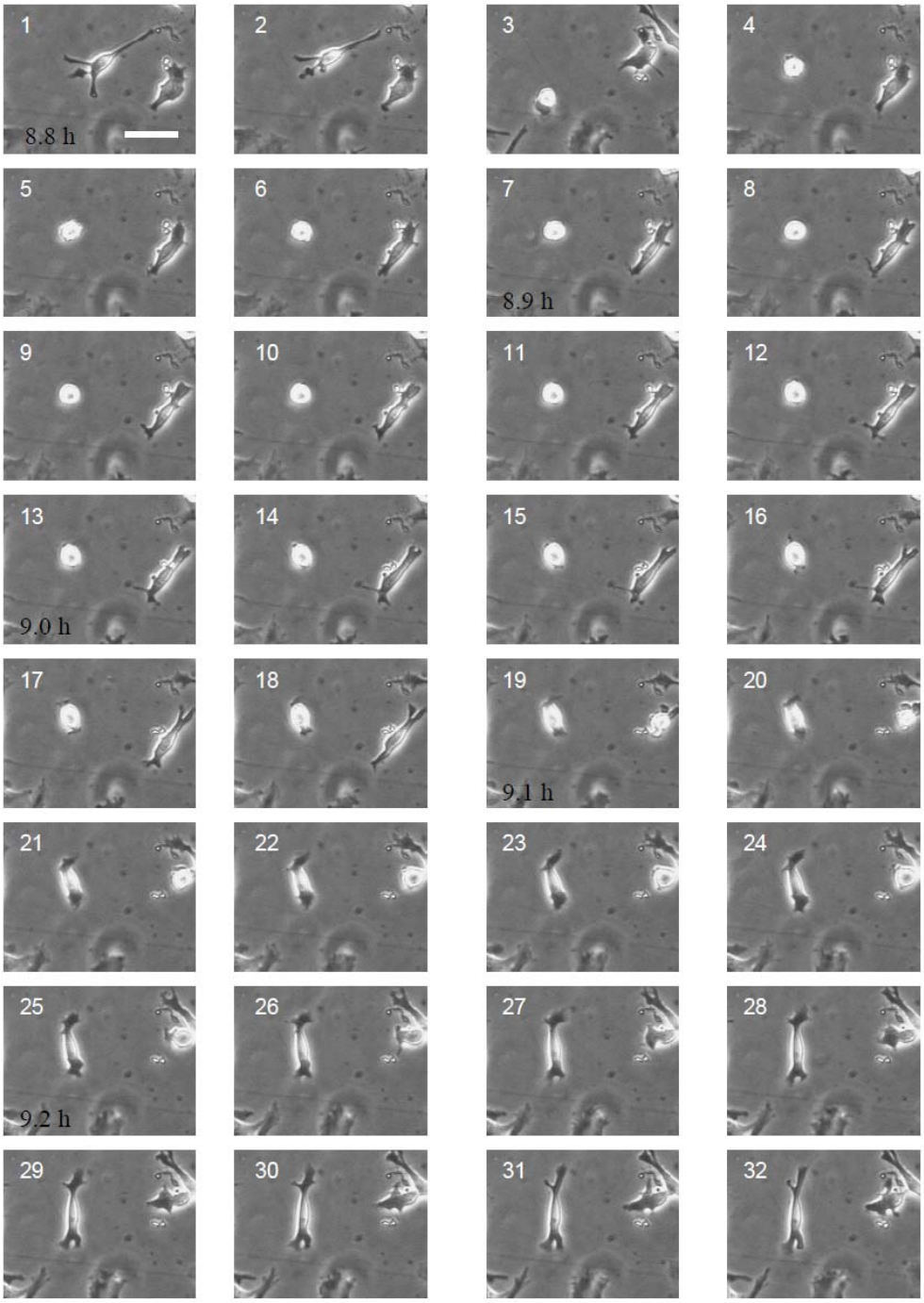
1
8.8 h
2
3
4
5
6
7
8.9 h
8
9
10
11
12
13
9.0 h
14
15
16
17
18
19
9.1 h
20
21
22
23
24
25
9.2 h
26
27
28
29
30
31
32

Figure 11b

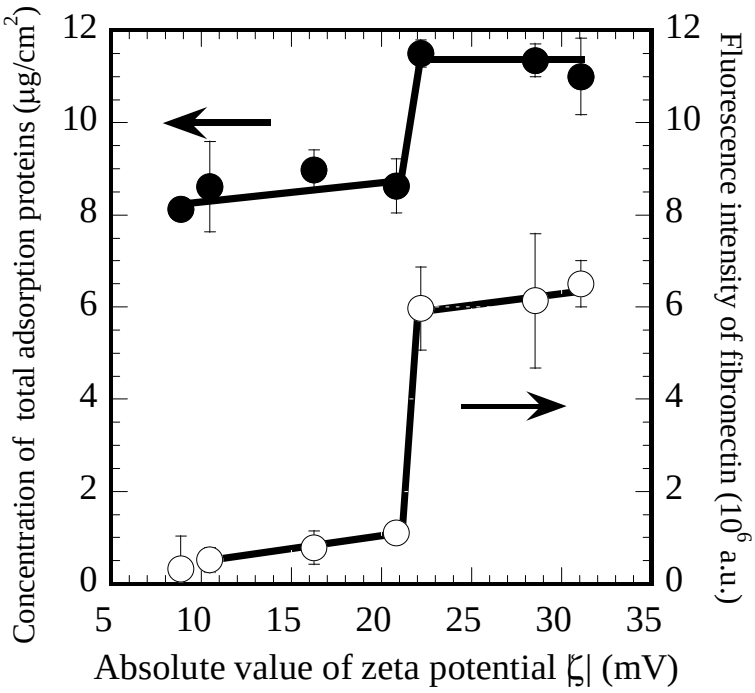
Concentration of total adsorption proteins (μg/cm²)
Fluorescence intensity of fibronectin (10⁶ a.u.)
Absolute value of zeta potential |ζ| (mV)
0
2
4
6
8
10
12
5
10
15
20
25
30
35

Figure 12

Hydrogels / Scaffolds	*M* (mol%)	Column I HUVEC	Column II Adhered platelet on HUVECs	D_p (10^4platelet /μm^2)
PAA	2	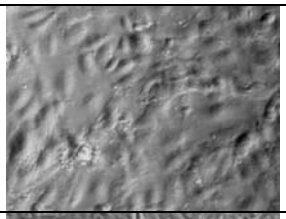	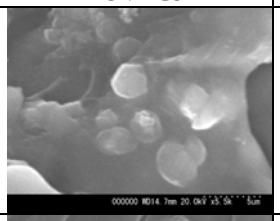	115
PNaAMPS	2	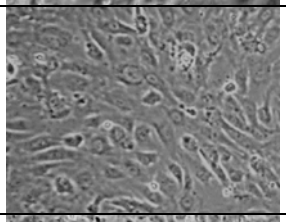	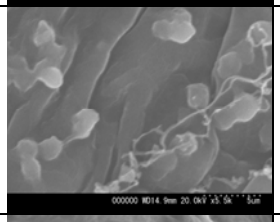	183
	10	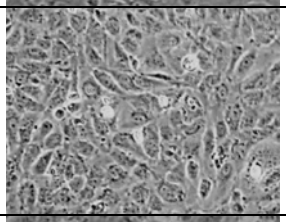	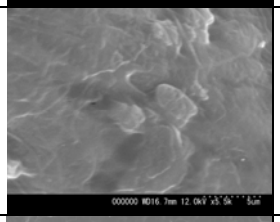	6
PNaSS	4	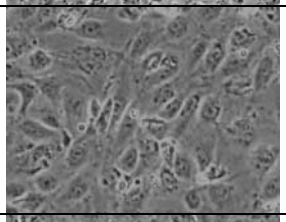	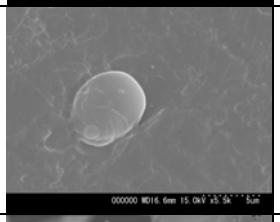	0
	10	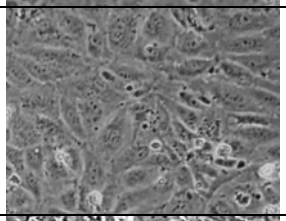	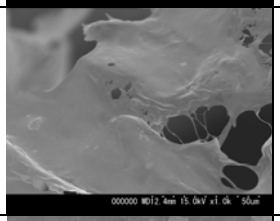	0
TCPS (Control)	/	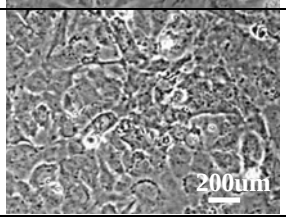	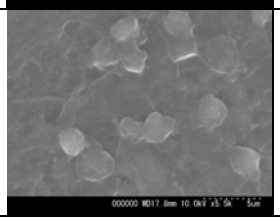	185

Figure 13

M (mol%)	E (kPa)	HCAEC monolayer	Adhered platelet on HCAECs	Relative RNA of core proteins in GAG			Relative amount of GAG	D_p (10^4platelet /μm^2)
				glypican	syndecan-4	perlecan		
4	3	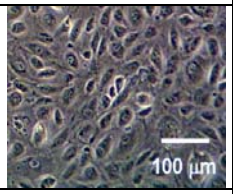	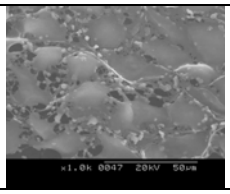	2.3	1.7	2.0	0.5	96
10	60	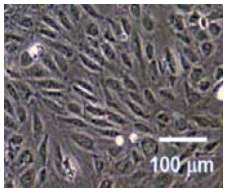	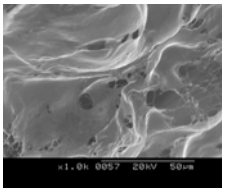	3.2	2.3	2.6	2.1	12
13	100	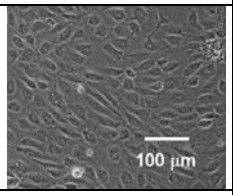	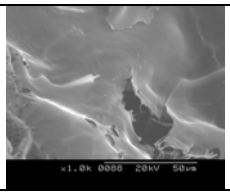	3.8	2.4	3.1	2.1	3
TCPS (Control)	3×10^6	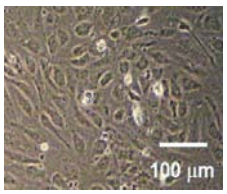	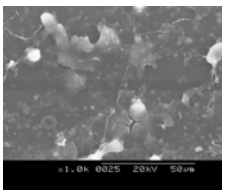	1	1	1	1	101

Figure 14

Table 1 Degree of swelling (*q*) of poly(NaAMPS-*co*-DMAAm) hydrogels in HEPES buffer solution. ($NaHCO_3$ 1.55×10^{-2} M, HEPES 5×10^{-3} M, NaCl 0.14 M, pH = 7.4)

Hydrogel \ F	0	0.05	0.1	0.2	0.3	0.4	0.5	0.7	1.0
poly(NaAMPS-*co*- DMAAm)	8.37±0.36	8.48±0.75	8.87±1.42	9.69±1.31	10.4±1.22	10.9±0.39	12.2±1.40	13.0±1.31	17.0±0.47